Continuous Shear Thickening and Colloid Surfaces

J. R. Melrose,[1] J. H. van Vliet,[1] and R. C. Ball[2]
[1]*Polymer and Colloid Group, Cavendish Laboratory, Cambridge, United Kingdom*
[2]*Theory of Condensed Matter Group, Cavendish Laboratory, Cambridge, United Kingdom*
(Received 17 August 1995; revised manuscript received 10 July 1996)

We elucidate the basic physics of shear thickening in colloids from the viewpoint of the dissipative interactions between close approaching particles. With just hard-sphere lubrication, Brownian spheres show a logarithmic thickening at high stresses. We use a model of interactions due to porous surfaces to show that thickening is enhanced by stronger dissipative surface forces, and compare successfully simulation with experiment. The onset of thickening is sensitive to the degree of order and history of shear. [S0031-9007(96)01743-7]

PACS numbers: 83.50.Qm, 82.70.Dd

Dense colloidal suspensions at high shear rates exhibit thickening effects: a rise of viscosity with increasing shear rate. At volume fractions approaching close packing, discontinuous thickening with a large jump in viscosity can occur at a critical stress; however, at lower volume fractions and lower stresses a more continuous rise is often reported. Many systems show thickening [1], including colloids of monodisperse spherical particles [2,3].

The microstructural origins of thickening are not resolved. Some have seen it as a general feature of nonequilibrium phase diagrams [4] resulting from an increase in particle Reynolds number, others as a mechanical instability of layered flow [5]. Some theories [2,5] emphasize the competition between conservative repulsive forces and hydrodynamic forces. Some have speculated on the role of Brownian forces [3,6,7] either as a source of mechanical instability of layer flow [7] or as relaxation mechanisms for clusters [3]. Thickening has been seen in a number of molecular dynamics simulations [4,8], but a simulation study of colloids [9,10] showed thickening and clustering due to divergent lubrication interactions.

In this Letter, we will show that thickening is particularly sensitive to the near field interparticle dissipative interactions. We point out that these interactions need be included to quantitatively understand experiment and that measurements of thickening are probes of these interactions.

We think that the fundamental origins of thickening in colloids is evident in the behavior of particle systems with only dissipative interactions. We have recently shown [11] that at high concentrations such systems do not reach a steady state under shear due to rapid collapse of interparticle gaps at low applied strains. A kinetic clustering theory [12] based on the shear induced growth of rigid rodlike clusters down the compression axis predicts this rapid collapse and defines a jamming transition at a volume fraction below close packing in which an infinite cluster gels at low strain before it can tumble. Such a jam is likely the origin of discontinuous shear thickening. In the presence of other interactions the onset of jamming is probably sensitive to both applied stress and volume fraction. This Letter will explore continuous thickening in which Brownian and conservative forces lead to steady states in regions outside that where jamming occurs.

We now introduce our simulation technique and particle models. Modeling the flow of particles concentrated in a hydrodynamic medium is a significant challenge. The most studied algorithm [9] involves $O(N^3)$ inversions of matrices [10]. In the limit of high shear rates and concentrated systems where shear thickening occurs, the divergent hydrodynamic interactions due to the relevant motion of the surfaces of close particles must dominate the resistance to particle motion. We retain just these near field, two-body terms in our model. Others have made a similar approximation [13,14] but the scope of our results is unprecedented.

For hard spheres, these near field dissipative interactions are well known. They can be divided into squeeze modes—the leading divergent interaction—along the line of centers and modes arising from the transverse motion of neighbors. To leading order in the intersurface gaps the Reynolds lubrication squeeze mode force on a particle i is given by

$$f_i = -\sum_j (3\pi\mu d^2/8h_{ij})[(\mathbf{v}_i - \mathbf{v}_j)\cdot\mathbf{n}_{ij}]\mathbf{n}_{ij} + O(\ln(2/h_{ij})), \quad (1)$$

where μ is the viscosity of the solvent, the sum is over nearest neighbor particles j, h_{ij} is the gap between the surfaces, $\mathbf{n}_{ij}$ is the unit vector along the line of centers i to j, and $\mathbf{v}_i, \mathbf{v}_j$ are the particle velocities. We included additional logarithmic nonanalytic terms [15] for the squeeze, shear, and rotation modes. The hydrodynamic, colloidal, and Brownian force and torque balance on each particle to give the equation of motion

$$-\mathbf{R}\cdot\mathbf{V} + F_C + F_B = 0. \quad (2)$$

The hydrodynamic force and torques $\mathbf{R}\cdot\mathbf{V}$ are related linearly to the $6N$ velocity/angular vector $\mathbf{V}$ by the

 0031-9007/96/77(22)/4660(4)$10.00

resistance matrix **R** formed from a sparse sum of terms such as (1). Flow is driven by Lee-Edwards periodic boundary conditions [16] on the velocity field. Nearest neighbors are identified by the construction of Delaunay tetrahedra [17]. Each time step, Eq. (2) was solved for **V** by conjugate gradient techniques (note inversion of **R** leads to a long-ranged and many body mobility matrix). We use a variable time step such that particles never overlap.

For Brownian simulations we generate random force and torque F_B on each particle through a sum of weighted pair terms on each bond such that they obey the fluctuation-dissipation theorem: $\langle F_B F_B \rangle = 2kTR$. Terms in the gradient of the diffusion tensor are included by use of an order δt^2 algorithm for the particle trajectory and the computation of stress at the half time step position leads to devatoric Brownian contributions.

In this Letter, we will use two models of the surfaces of colloid particles. The first is Hookian spheres with conservative repulsive forces represented by linear repulsive springs around a hydrodynamic hard sphere with dissipative interactions given by (1). Between particles i and j separated by r_{ij} the spring force is

$$\mathbf{f}_{ij}^{c}(r) = -\mathbf{n}_{ij}[F_0 - (F_0/\delta_c)r_{ij}] \quad \text{if } r < \delta_C\,. \tag{3}$$

Note $\delta_c/2$ sets how much the thermodynamic volume fraction Φ_T, that measured by the second virial coefficient, exceeds Φ, that set by the divergence of (1). We define a dimensionless spring constant $K = (F_0/\delta_c)/(\dot{\gamma}\mu d)$, where $\dot{\gamma}$ is the applied shear rate, and a dimensionless shear rate W:

$$W = \dot{\gamma}\mu d^2/F_0\,. \tag{4}$$

For stiff springs, $W \ll 1$, these set a minimum gap between particles at δ_c. We mimic a dissipative surface layer (see below) by introducing an *ad hoc* power law divergence to the viscosity inside δ_c by simply multiplying (1) and the shear terms by a factor

$$1 + (h_{ij}/\delta_c)^{\beta} \quad \text{for } h_{ij} < \delta_c \tag{5}$$

The linear springs have a maximal compressive load which when exceeded determines a collapse of the spring into the regime of enhanced dissipation.

The second model we take from the literature [18,19]. It models a porous polymer coat on particles. The conservative part of this interaction has the form

$$\mathbf{f}_{ij}^{c}(r) = -Q(kT/d)\mathbf{n}_{ij}[(2\delta_c)^{-5/4} - (h_{ij})^{-5/4}], \quad \text{if } r < \delta_c\,. \tag{6}$$

The scale parameter $Q = 2\Pi\kappa[(\Gamma d^2)^{9/4}(a/d)^{15/4}]$ with Γ the number of chains per unit area, a the polymer monomer size, and κ a constant; here we will quote Q as a single lumped parameter.

The dissipative part is that of fluid flow through a polymer coat described by the Brinkman equation—this enhances the dissipation over (1). An expression has recently been given [19]. The strength of the dissipative force is controlled by a nominal porosity length scale ξ_p (strictly within the original model, this is related to the polymer correlation length of the coat; however, here we allow it to vary independently). Figure 1 shows a plot of the squeeze mode of this interaction; it is overall stronger than (1) but while around the regime of contact of the coats this force grows more steeply than (1), in the regime of compressed coats its divergence is weaker than (1). There are other physical mechanisms which may lead to viscous interactions differing from (1)—but we ignore these.

First, we report on thickening of Brownian and Hookian hard spheres with Reynolds lubrication (1). By applying conditions in which the particles under flow approach ever closer, in one case with a shortening of the surface spring and in the other by increasing the stress, we find a thickening which varies as a logarithm of the inverse of the interparticle gap. Figure 2 shows the hydrodynamic contribution to the viscosity from simulations at volume fractions $\Phi = 0.48$ and 0.51. For Brownian spheres this is plotted against the stress while for the Hookian spheres it is plotted against $(1/\delta_c)$ where a stiff spring $K = 10^6$ is set buts its length varied as a direct control of the interparticle gaps. In the latter case, the viscosity increases despite a decrease in thermodynamic phase volume. In the Brownian case, the inverse dimensionless stress is also a length scale δ_B, characteristic of close approach. Equating the Brownian forces between a pair of particles kT/δ_B to that due to the

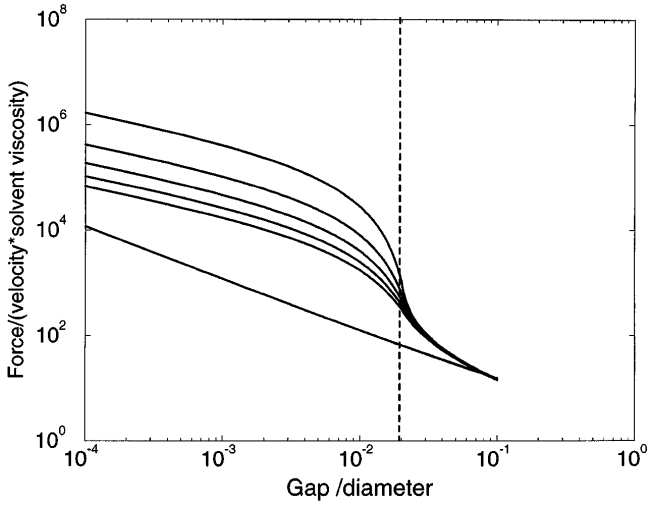

FIG. 1. The dissipative force law of Refs. [19,20] and Eq. (1) of the text plotted against the gap between a pair of particles. The force is divided by the product of the relative velocity down the line of centers and solvent viscosity. Curves bottom to top: Eq. (1), then with coats 0.01 diameters thick and $\xi_{p/d} = 0.001,\ 0.0008,\ 0.0006, \ldots, 0.0002$ diameters; the vertical line indicates contact of the coats.

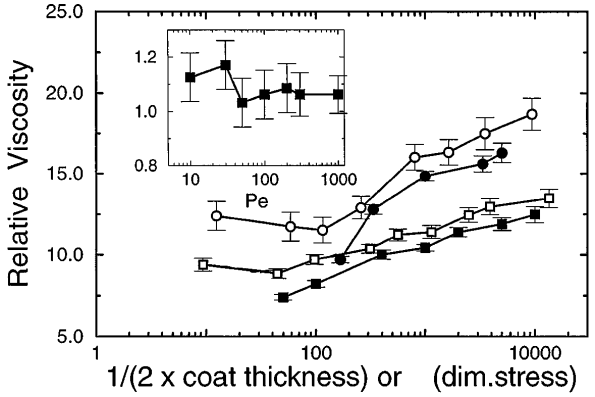

FIG. 2. Thickening effects at $\Phi = 0.48$ (squares), 0.51 (circles) the hydrodynamic contribution to the viscosity plotted against η_H Pe for Brownian spheres (closed symbols) and $1(2\delta_c/d)$ for Hookian spheres (open symbols). Inset: the prediction (7) for the peak position in ratio to that in the actual distribution plotted against Peclet.

hydrodynamic shear stress $\sigma_H d^2$, where d is the particle diameter, determines

$$\delta_B/d \approx kT/\sigma_H d^3 \approx 1/\eta_H \mathrm{Pe}\,, \tag{7}$$

where we have introduced the shear rate Pe as the Peclet number and η_H the hydrodynamic contribution to the viscosity relative to that of the solvent (δ_B/d is the boundary layer thickness where convection and diffusion balance). We examined the distribution of the gaps between nearest neighbors. For Pe $>$ about 10 a broad peak appears in this distribution at small gaps and becomes more distinct the higher Pe. In the inset of Fig. 2 we plot $1/\eta_H$ Pe divided by the gap at this peak—the data corroborate (7). Over the range we are able to study, the viscosity increases, but only logarithmic with Peclet. Note, there is no true second Newtonian plateau in the data—even large Pe is relevant. Although we cannot rule out that the viscosity increase diminishes at even higher rates, it is a common misunderstanding that Brownian effects are irrelevant at high shear rates. Similar conclusions have been reached by the authors of Refs. [9,10]. We find that varying repulsive conservative forces does not enhance the logarithmic thickening of (1).

We now compare data for real colloids. In Fig. 3 we show data for experiments on PMMA particles with PHS polymer coats [3] in two different solvents and silica particles [20] all circa 0.5 core volume fraction. For the PMMA particles, one of the solvents (II) was a poor solvent for the coat and this system shows a strong shear thickening response (open circles and squares). We coplot simulations of Brownian spheres with (1) and simulations with coats of thickness 0.01 (the order of the thickness of the PHS coats) and porosity 0.0005 diameters but differing strengths $Q = 50, 10kT/d$ and compare with the experimental data set at the volume fraction 0.49 in the poor solvent (II). It is clear that the gradual thickening of Brownian hard spheres with Reynolds lubrication cannot explain the experiment in solvent II—but the coat model with $Q = 50kT/d$ does produce a thickening response quantitatively comparable. We do not claim to have shown that the particular coat interaction is appropriate for the particular system [3]—although we do use a conservative force comparable to that measured [3] and the porosity is of the order of the interchain spacing for the system [3]. We have not examined the effect of changing the solvent quality directly. This will change the coat thickness, porosity, and strength simultaneously leading to a complex sensitivity which cannot be understood by simple scaling arguments (it may also change the surface roughness which current models do not account for). We do conclude, however, that dissipation at contacting surfaces enhanced relative to that of hard spheres is necessary to explain the degree of thickening in experiment and sufficiently described by the coat model.

There have been no previous predictions of rheology in 3D reported at this volume fraction with polymer coat models. In the shear thinning regime, the simulation data lie in between the experiments both quoted at 0.5 volume fraction. It is interesting to note the sensitivity to the coat interaction in the thinning regime. The logarithmic thickening of the Brownian spheres is in contrast to the high shear rate Newtonian plateau of the experiment in solvent I. However, such plateaus may be due to coats; it is recovered in the simulations (Fig. 3) with coats in the regime where the conservative forces are strong relative to the applied shear forces.

Finally, we examine the role of order under flow in thickening. Under flow, order exists for stiff and thick enough surface "springs." The thickening regimes of Fig. 3 are associated with a decline in order with increasing thickening—interestingly this is gradual throughout the thickening regime rather than a sharp order-disorder transition at the onset of thickening. At lower volume fractions we can observe thickening in regimes without order. We use the Hookian spheres to illustrate different scenarios. With this model, if particles are pushed together such that the maximal force F_0 is exceeded, then this determines a sharp transition to viscous contacting surfaces with $\beta > 0$ and thickening. In the inset of Fig. 3 we fixed $\delta_c/d = 0.01$ and $\beta = 4$ and varied the shear rate W at $\Phi = 0.55$ and 0.48. At $\Phi = 0.55$ the system is ordered under flow. If this system is sheared at a sequentially increasing rate, then it is shear thinning up to the onset of thickening. The transition point, however, is history dependent: Starting each run from a disordered rest state leads to an earlier onset. This occurs because stress concentration in disordered starting states is higher than in the ordered steady state. In contrast, at $\Phi = 0.48$ the system prior to thickening is disordered under flow and the sudden thickening is preceded by a gradual thickening. These different scenarios are a feature of experiment [3].

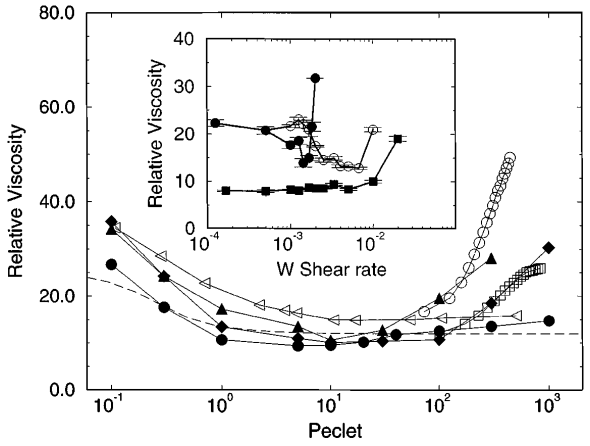

FIG. 3. Simulations of $N = 50$ Brownian spheres at $\Phi = 0.5$: Brownian spheres with Eq. (1) (filled circles). Spheres with the interactions of Ref. [18], and coat thickness 0.01 diameters; effective pore size 0.0005 diameters and osmotic force strength [see Eq. (7)] $Q = 10$ (filled triangles), 50 kT/d (filled diamonds). Experiments: 690 nm particles of Ref. [3] in solvent II and volume fraction 0.51 (0.49) unfilled circles (squares); 1200 nm particles in solvent I (unfilled triangles). Dashed line Ref. [19] Inset: viscosity against W for spring coated spheres with $\delta_c/d = 0.01$ at $\Phi = 0.48$ (squares), 0.55 (circles). The closed symbols were from a fresh rest configuration at each shear rate, while the open symbols were simulated under stepwise increase of shear rate.

Our view of thickening is that it is due to the close approach of particles with strong dissipative interactions. We differentiate between jamming and continuous thickening. In the former case rigid percolating clusters exist, but in the latter case any connection between thickening and the formation of finite rigid clusters remains to be clarified. Both conservative and Brownian forces may control the length scales of close approach of particles and hence the degree to which near field dissipation is felt. The former may set a critical stress above which particle pairs contact with high dissipation—this may lead to a jump to new steady state with higher viscosity or even jamming. Thickening is not in principle an order-disorder effect—it can occur out of disordered flow regimes. Our results indicate that models without inertia are sufficient to explain thickening in colloid systems.

More generally, we note that the above and other results suggest to us that *concentrated* colloids in *shear flow* can quite successfully be modeled with $O(N^2)$ simulation techniques with just the divergent hydrodynamic interactions. This opens the prospect of systematic quantitative studies of the role of particle surfaces in the bulk rheology of concentrated colloids.

We thank S. F. Edwards, A. Lips, R. Buscall, A. Rennie, S. Clarke, L. Silbert, and, in particular, W. Frith, R. Farr, and J. Brady for many useful discussions. We thank the authors of Ref. [3] for allowing us to include some of their data. We thank the DTI/colloid technology project cofunded by the DTI, Unilever, Schlumberger, and ICI, the Colloid Hydrodynamics Grand challenge project, and the BBSRC food directorate for funding.

[1] H. A. Barnes, J. Rheol. **33**, 329 (1989).
[2] W. H. Boersma, J. Laven, and H. H. Stein, AIChE J. **36**, 321 (1990); J. Colloid Interface Sci. **149**, 10 (1992); M. K. Chow and C. F. Zukoski, J. Rheol. **39**, 15, 33 (1995).
[3] P. d'Haene, Ph.D. thesis, Catholic University, Leuvan, 1993; W. J. Frith, P. d'Haene, R. Buscall, and J. Mewis, J. Rheol. **40**, 531 (1996). The systems in these works is PMMA (polymethylmethacrylate) particles with PHS (polyhydrox steric acid) polymer coat in solvents: (I) decalin and (II) DOP (didodecylphyhalate).
[4] L. V. Woodcock, Chem. Phys. Lett. **111**, 455 (1984).
[5] R. L. Hoffman, J. Colloid Interface Sci. **46**, 491 (1974).
[6] A. B. Metzner and M. Whilock, Trans. Soc. Rheol. **11**, 329 (1958).
[7] G. N. M. Choi, Ph.D. thesis, University of Michigan, 1983.
[8] D. M. Heyes, J. Chem. Soc. Faraday Trans. **82**, 1365 (1986).
[9] G. Bossis and J. F. Brady, J. Chem. Phys. **80**, 5141 (1984); J. F. Brady, R. J. Phillips, J. C. Lester, and G. Bossis, J. Fluid. Mech. **195**, 257 (1988), and references therein.
[10] T. N. Phung and J. F. Brady, in *Slow Dynamics in Condensed Matter*, edited by K. Kawasaki, M. Tokuyama, and T. Kawakatsu AIP Conf. Proc. No. 256 (AIP, New York, 1992); T. N. Phung, Ph.D. thesis, California Institute of Technology, 1993.
[11] R. C. Ball and J. R. Melrose, Adv. Colloid Interface Sci. **59**, 19 (1995); Europhys. Lett. **32**, 535 (1995).
[12] R. Farr, R. C. Ball, and J. R. Melrose (unpublished).
[13] N. A. Frankel and A. Acrivos, Chem. Eng. Sci. **22**, 847 (1967); B. H. H. A. van der Brule and R. J. J. Jongschaap, J. Stat. Phys. **62**, 1225 (1991).
[14] M. Doi, D. Chen, and K. Saco, in *Ordering and Organising in Ionic Solutions* (World Scientific, Singapore, 1987), p. 482; M. Toivakka, D. Eklund, and D. W. Bousfield, J. Non-Newton Fluid Mech. **56**, 49–64 (1995).
[15] S. Kim and S. J. Karrila, *Microhydrodynamics* (Butterworths, London, 1992).
[16] A. W. Lees and S. F. Edwards, J. Phys. C **5**, 1921 (1972).
[17] R. C. Ball and J. R. Melrose (unpublished).
[18] G. H. Fredrickson and P. Pincus, Langmuir **7**, 786 (1991).
[19] A. A. Potanin and W. B. Russel, Phys. Rev. E **52**, 730 (1995).
[20] J. C. van der Werf andC. G. de Kruif, J. Rheol. **33**, 421–454 (1989). In Fig. 3 we plot the fit function of this reference for the parameters of silica particles SJ18 at volume fraction 0.506.